Published in final edited form as:
Biomaterials. 2013 December ; 34(38): . doi:10.1016/j.biomaterials.2013.08.082.

Human Progenitor Cell Recruitment via SDF-1α Coacervate-laden PGS Vascular Grafts

Kee-Won Lee[a], **Noah R. Johnson**[a], **Jin Gao**[a], and **Yadong Wang**[a,b,c,d,*]

[a]Department of Bioengineering, University of Pittsburgh, Pittsburgh, PA 15261, USA

[b]Department of Chemical Engineering, University of Pittsburgh, Pittsburgh, PA 15261, USA

[c]Department of Surgery, University of Pittsburgh, Pittsburgh, PA 15261, USA

[d]McGowan Institute for Regenerative Medicine, University of Pittsburgh, Pittsburgh, PA 15261, USA

Abstract

Host cell recruitment is crucial for vascular graft remodeling and integration into the native blood vessel; it is especially important for cell-free strategies which rely on host remodeling. Controlled release of growth factors from vascular grafts may enhance host cell recruitment. Stromal cell-derived factor (SDF)-1α has been shown to induce host progenitor cell migration and recruitment; however, its potential in regenerative therapies is often limited due to its short half-life *in vivo*. This report describes a coacervate drug delivery system for enhancing progenitor cell recruitment into an elastomeric vascular graft by conferring protection of SDF-1α. Heparin and a synthetic polycation are used to form a coacervate, which is incorporated into poly(glycerol sebacate) (PGS) scaffolds. In addition to protecting SDF-1α, the coacervate facilitates uniform scaffold coating. Coacervate-laden scaffolds have high SDF-1α loading efficiency and provide sustained release under static and physiologically-relevant flow conditions with minimal initial burst release. *In vitro* assays showed that coacervate-laden scaffolds enhance migration and infiltration of human endothelial and mesenchymal progenitor cells by maintaining a stable SDF-1α gradient. These results suggest that SDF-1α coacervate-laden scaffolds show great promise for *in situ* vascular regeneration.

Keywords

Coacervate; Polycation; Stromal cell-derived factor (SDF)-1α; Poly(glycerol sebacate); Human progenitor cells; Tissue engineering

1. Introduction

Tissue-engineered vascular grafts have been developed as arterial substitutes to overcome limitations of autografts and synthetic grafts. Tissue-engineered vascular grafts are typically cell-based, consisting of a biomaterial scaffold seeded with vascular cells [1, 2] or scaffold-

*Corresponding author: 3700 O'Hara Street, Pittsburgh, PA 15261, USA, Tel) +1 412 624 7196; Fax) +1 412 524 3699; yaw20@pitt.edu.

less vascular cell sheets [3]. Despite significant progress, these approaches require harvesting vascular cells and months of *in vitro* cell culture, which may limit potential clinical use. Graft integration within the host is also a challenge for designing an effective tissue-engineered vascular graft. Recently, decellularized allogeneic tissue-engineered arteries have been developed as readily available grafts [4, 5], but they require *in vitro* isolation and expansion of recipient endothelial cells for seeding, which is not cost or time-effective. Seeding biodegradable scaffolds with bone marrow cells, which are easily obtained and immediately available, overcame these limitations in clinical trials [6, 7]. However, these grafts were implemented at low pressure sites such as the pulmonary artery or vein, not in high pressure systemic circulation.

Cell-free approaches to vascular grafts address the issues associated with donor site morbidity, time, and cost by completely avoiding cell harvesting and *in vitro* culture. Previous studies have shown that neovessels following graft implantation are host-derived [8], the source of which may be circulating blood or adjacent vessels [9]. Cell-free vascular grafts exploit this host cell infiltration, which abrogates the need for exogenous cell seeding prior to graft implantation. We have recently shown degradable vascular grafts can rely on host cells to regenerate arteries *in situ* without prior cell seeding [10]. One key source of host cells are vascular progenitor cells including endothelial progenitor cells (EPCs) and mesenchymal progenitor cells (MPCs). It is known that EPCs originate from bone marrow-derived cells circulating in peripheral blood [11], and these cells are a promising autologous source for replacing arterial endothelial cells in tissue-engineered vascular grafts [12-14]. In addition, previous studies have reported the formation of functional microvascular beds by co-injection of EPCs and MPCs isolated from human cord blood and bone marrow [15, 16]. These findings demonstrate the importance of recruitment of host EPCs and MPCs in the development of tissue-engineered vascular grafts. Since host cell infiltration proceeds faster in rodent models than in humans, we anticipate a great need to accelerate host cell infiltration for clinical translation of cell-free approaches in tissue engineering vascular grafts.

Stromal cell-derived factor (SDF)-1α is a promising chemoattractant of host EPCs and MPCs because it induces host progenitor cell mobilization and recruitment by binding to CXC chemokine receptor type 4 (CXCR4) [17-19]. However, SDF-1α has a short half-life in the bloodstream [20] and is prone to degradation by matrix metalloproteinases which are activated at sites of injury [21]. Thus, a delivery system to stabilize SDF-1α and provide long-term sustained release is crucial for its *in vivo* efficacy. Several such delivery systems have been developed by incorporating SDF-1α into various matrices such as polymeric scaffolds [22-25], hydrogels [26-29], and nanoparticles [30]. These previous delivery systems have demonstrated benefits for progenitor cell recruitment; however, deficiencies such as low loading efficiency and high initial burst release may limit their long-term efficacy.

Here, we report a new SDF-1α delivery system to enhance progenitor cell recruitment for vascular graft remodeling. The design of our delivery system was based on three main criteria: SDF-1α protection and release, scaffold construction, and scaffold porosity. First, to protect SDF-1α and support its long-term sustained release, we used a charge-based self-assembled coacervate containing intact heparin and a synthetic polycation, poly(ethylene argininylaspartate diglyceride) (PEAD) (Figure 1). We previously reported that this coacervate can control the release of growth factors and maintain their bioactivities [31]. Recently, we demonstrated that coacervate-delivered basic fibroblast growth factor (FGF-2) enhanced angiogenesis after injection subcutaneously or into the infarcted myocardium [32, 33], and coacervate-delivered heparin-binding EGF-like growth factor (HB-EGF) accelerated closure of full-thickness skin wounds [34]. Second, to provide an elastomeric

matrix for the vascular cells, we used poly(glycerol sebacate) (PGS) scaffolds. PGS is a tough, biodegradable elastomer with excellent mechanical properties and biocompatibility for tissue engineering [35]. Third, to provide an open porous structure for cell retention and migration, we used salt leaching to fabricate scaffolds with interconnected micro- and macro-pores [36]. This scaffold design enabled rapid host remodeling and constructed neoarteries at 3 months post-implantation [10]. To assess progenitor cell recruitment of our delivery system, we used human endothelial and mesenchymal progenitor cells, and examined their migration and infiltration using *in vitro* assays.

2. Materials and methods

2.1. Preparation of SDF-1α coacervate

PEAD was synthesized as previously described [31]. Heparin from porcine intestine (Scientific Protein Labs, Waunakee, WI) and PEAD were each dissolved at 10 mg/mL in deionized (DI) water and sterilized with a 0.22 μm syringe filter. Heparin was combined with recombinant human SDF-1α (PeproTech, Rocky Hill, NJ). PEAD was then added (5:1 mass ratio of PEAD:heparin) which immediately induced coacervation.

2.2. Cell isolation, culture, and characterization

Human cord blood-derived endothelial progenitor cells (cbEPCs) and bone marrow-derived mesenchymal progenitor cells (bmMPCs) were generously supplied from Dr. Joyce Bischoff in Boston Children's Hospital at Harvard Medical School. The isolation and expansion of both cell types have been previously described in detail [15]. The cbEPCs were cultured on fibronectin-coated (1 μg/cm^2; Chemicon International, Temecula, CA) plates using EPC medium: endothelial basal medium-2 (Lonza, Walkersville, MD) supplemented with 20% fetal bovine serum (Hyclone, Logan, UT), 1% L-glutamine-penicillin-streptomycin (Mediatech, Manassas, VA), and endothelial growth medium-2 SingleQuot Kit (Lonza) (except hydrocortisone). The bmMPCs were grown on fibronectin-coated plates in MPC medium, which is identical to EPC medium but does not contain vascular endothelial growth factor (VEGF), basic fibroblast growth factor (bFGF), and heparin.

Both progenitor cell types were characterized by immunofluorescent staining of CXC chemokine receptor type 4 (CXCR4). Cells (passage 8) were plated in a 24-well plate at a density of 10,000 cells/cm^2 in 500 μL of culture medium and incubated at 37°C for 24 h. Cells were then fixed in 4% paraformaldehyde for 10 min, blocked with 5% normal goat serum (Sigma-Aldrich, St. Louis, MO) for 1 h at 37 °C, incubated with rabbit polyclonal anti-CXCR4 (1:100; Abcam, Cambridge, MA) primary antibody for 45 min at 37°C, and incubated with Alexa Fluor 488 goat anti-rabbit IgG (1:200; Invitrogen, Carlsbad, CA) secondary antibody for 45 min at 37°C. Nuclei were stained with 4′,6-diamidino-2-phenylindole (DAPI) (Invitrogen).

2.3. Transwell chemotaxis assay

cbEPCs and bmMPCs (passage 8) were seeded in 8 μm pore size transwell inserts (Millipore, Billerica, MA) at a density of 10,000 cells/cm^2. Three groups were applied in the study: (1) basal medium (as a negative control): medium without supplemental growth factors, (2) delivery vehicle: basal medium containing coacervate (heparin:PEAD = 5 μL:25 μL) only, and (3) SDF-1α coacervate: basal medium containing the coacervate loaded with 1, 2, 5, and 10 μL of SDF-1α (50 ng/μL). Compositions of each group are listed in Table 1. After incubation for 6 h, non-migrated cells were removed with cotton swabs. Migrated cells were fixed with methanol for 10 min and stained with Quant-iT PicoGreen dsDNA reagent (Invitrogen). Fluorescent images were captured using an inverted microscope (Eclipse T*i*-E, Nikon Instruments, Melville, NY). Migrated cells were counted from images taken in three

different areas per group and normalized by the total number of cells in the basal medium group.

2.4. Fabrication of PGS scaffolds

Flat and tubular scaffolds were fabricated from a biodegradable elastomer, poly(glycerol sebacate) (PGS) [35] using a previously described salt fusion/leaching method [36, 37]. Ground salt particles with diameters of 75-150 μm were used as porogens. The final dimensions of the PGS scaffolds were 40 mm diameter and 0.8 mm thickness (for flat scaffolds), and 40 mm length, 6 mm outer diameter, and 0.5 mm wall thickness (for tubular scaffolds). The theoretical porosity of both scaffolds was 80%.

2.5. Incorporation of SDF-1α coacervate

SDF-1α was labeled with Alexa Fluor 488 Microscale Protein Labeling Kit (Molecular Probes, Eugene, OR) following the manufacturer's instruction to examine distribution within the PGS scaffolds. The coacervate was formed by combining 10 μL of heparin solution with 2 μL of Alexa Fluor 488-labeled SDF-1α (50 ng/μL), followed by addition of 50 μL of PEAD solution. Both flat and tubular scaffolds were coated with the coacervate by dropping or injecting it onto the surface and lumen of the scaffolds, then air-drying for 30 min. The surface morphology of coacervate-coated scaffolds was examined using a field emission scanning electron microscope (6330F, JEOL, Tokyo, Japan). SDF-1α coacervate distribution in the scaffolds was visualized with fluorescence microscopy. Briefly, coacervate-coated scaffolds were embedded in Tissue-Tek optimal cutting temperature compound (Sakura Finetek, Torrance, CA), snap-frozen with dry ice, and cryosectioned to give 10 μm thick sections. Slides were viewed with an inverted microscope (Nikon).

2.6. SDF-1α loading efficiency and release profile

Loading efficiency and release profiles were measured using radio-labeled SDF-1α. The coacervate was formed as described above using ^{125}I-labeled human recombinant SDF-1α (0.1 ng/μL) (PerkinElmer, Waltham, MA). Scaffolds were coated with the coacervate and soaked in 500 μL of PBS for 1 min, then the supernatant was collected. The radioactivity of collected supernatants was measured using a Packard Cobra II Gamma Counter (PerkinElmer) and normalized by that of a control solution containing the initial concentration of SDF-1α. The loading efficiency of SDF-1α was calculated as [1 – (radioactivity of the collected supernatants / radioactivity of the control solution)] × 100 (%).

The *in vitro* release of SDF-1α was assessed at pre-determined time points under both static and flow conditions. For static release experiments, SDF-1α coacervate-coated flat scaffolds (8 mm diameter, 0.8 mm thickness) were incubated in 500 μL of PBS at 37°C. On days 1, 4, 7, 14, 21, 28, and 35, the PBS supernatants were collected and replaced with fresh PBS. The radioactivity of collected supernatants was measured by the gamma counter to determine the amount of SDF-1α released from the scaffolds. For release experiments under flow condition, a custom designed bioreactor [37] was used to attach the scaffolds and circulate PBS at a constant flow rate. SDF-1α coacervate-coated tubular scaffolds were connected to the luminal silicon tubing of bioreactor chambers and a peristaltic pump supplied PBS from the reservoir at a flow rate of 8 mL/min (shear stress = ∼ 13 dyne/cm^2). At the same time points as static release experiments, 500 μL of PBS was collected from the reservoir and replaced with fresh PBS. The radioactivity of collected PBS was measured by the gamma counter. All SDF-1α release data were normalized to the radioactivity of a control solution containing the initial concentration of SDF-1α.

2.7. Cell migration assay using fibrin gel

Upward migration of fluorescence-labeled progenitor cells through a fibrin gel stimulated by SDF-1α released from coacervate-coated scaffolds on top of the gel was evaluated. cbEPCs and bmMPCs (passage 8) were labeled with CellTracker Red (CMTRX) and Blue (CMAC, Molecular Probes), respectively. Fibrinogen and thrombin from bovine plasma (Sigma-Aldrich) were dissolved at 3 mg/mL (fibrinogen) and 1 mg/mL (thrombin) in sterile PBS. Fluorescence-labeled cells were centrifuged at 1000 rpm for 5 min and resuspended with pre-warmed fibrinogen solution. Fibrin gels were formed by adding 20 μL of thrombin solution and 380 μL of cell-fibrinogen solution sequentially to each well in a glass chamber slide (Millipore), with each gel containing 10,000 cells. After gelation at 37°C for 10 min, SDF-1α coacervate (heparin:SDF-1α:PEAD = 10 μL:2 μL:50 μL)-laden (SDF-1α group) and empty (control group) ethylene oxide-sterilized flat PGS scaffolds were placed on the top surface of fibrin gels, and 200 μL of basal medium was overlaid onto the gel. On days 1, 4, and 7, overlaid medium was aspirated, the scaffolds were removed and the gels were imaged using a fluorescence microscope (Nikon). Optical sections were taken at 25 μm slice thickness along the z-axis of the gels and all images captured were reconstructed into three-dimensional (3D) volumetric images using the z-stack function. The number of cells in each gel were counted in the compiled images in 200 μm slice thicknesses from the bottom of the gel to the top and normalized by the total number of cells in the entire gel. To compare the number of migrated cells in both groups, the final normalized cell numbers at each depth in the SDF-1α group were divided by those in the control group and represented as a fold difference. All measurements were performed on three reconstructed 3D images per gel using NIS-Elements software (Nikon).

2.8. Cell recruitment assay

Both cbEPCs and bmMPCs (passage 8) were suspended in basal medium and 5,000 cells of each type were plated together on ultra-low attachment 24-well plates (Corning, Corning, NY). Three groups were used to assess progenitor cell recruitment: (1) empty scaffold (as a negative control), (2) free SDF-1α-loaded (SDF-1α:DI water = 2 μL:60 μL) scaffold, and (3) SDF-1α coacervate (heparin:SDF-1α:PEAD = 10 μL:2 μL:50 μL)-laden scaffold. Scaffolds were “skewered” on the end of a sterile 20G needle (BD, Franklin Lakes, NJ) and suspended in the well using a flat piece of silicone rubber. All well-plates were placed on an orbital shaker in a 37°C incubator and rotated at 4 rpm to avoid cell aggregation. On days 1, 4, 7, and 10, scaffolds were removed and bisected by razor blade for analysis.

2.8.1. Immunofluorescence staining—The presence of progenitor cells in the scaffolds was examined using immunofluorescence staining. Scaffolds were embedded in Tissue-Tek optimal cutting temperature compound (Sakura Finetek), snap-frozen in dry ice, and sectioned at 8 μm thickness. For cbEPC staining, mouse anti-human CD31 (1:50; Santa Cruz Biotech, Dallas, TX) primary antibody was used, followed by Alexa Fluor 594 goat anti-mouse IgG (1:100; Invitrogen) secondary antibody. For detection of bmMPCs, mouse anti-human CD90 (1:50; Millipore) primary antibody was used, followed by an Alexa Fluor 488 goat anti-mouse IgG antibody (1:100; Invitrogen). Nuclei were counterstained with DAPI.

2.8.2. PicoGreen DNA assay—One half of each scaffold from the cell recruitment assay was analyzed for DNA content. Scaffold wet weight was recorded, then the scaffold was cut into small pieces (1.0 mm^3), lysed in 250 μL of cell lysis solution (0.2 v/v % Triton X-100, 10 mM Tris pH 7.0, and 1 mM EDTA) for 30 min at room temperature, and centrifuged at 10,000 rpm for 10 min at 4°C. Double-stranded DNA (dsDNA) content of lysates was quantified using a Quant-iT PicoGreen dsDNA assay kit (Invitrogen) according to the

manufacturer's instructions and compared to the λ-DNA standard curve. The final dsDNA content of scaffolds was normalized to the wet weights of the scaffolds.

2.9. Statistical analysis

All results were reported as mean ± standard deviation. One-way analysis of variance (ANOVA) followed by Tukey's HSD post-hoc test was performed to assess statistically significant differences ($p < 0.05$) among groups using Minitab software (Minitab Inc., State College, PA).

3. Results

3.1. Characterization and chemotaxis of progenitor cells

We first characterized progenitor cells for CXCR4 expression and then evaluated the chemotaxis induced by SDF-1α coacervate at varying concentrations using a transwell assay. Immunofluorescent staining confirmed that both cbEPCs and bmMPCs displayed CXCR4 chemokine receptor (Figure 2A). Fluorescent images of transwell insert membranes showed enhanced chemotaxis of progenitor cells towards the coacervate with increasing SDF-1α dosages (Figure 2B). For cbEPCs, there was no significant difference in cell migration between the coacervate delivery vehicle alone (DV) and 50 ng of SDF-1α coacervate, but for SDF-1α dosages of 100 ng and greater, the number of migrated cells significantly increased (Figure 2C). bmMPC migration followed a similar trend, but was slightly lower than that of cbEPCs at the same concentrations of SDF-1α (Figure 2D). These results demonstrate that SDF-1α released from the coacervate can induce chemotaxis of both cbEPCs and bmMPCs. Based on these results, we used an SDF-1α dosage of 100 ng in subsequent experiments.

3.2. SDF-1α coacervate in PGS scaffolds

To examine incorporation and distribution of SDF-1α coacervate in the PGS scaffolds, we used SEM and fluorescence microscopy (Figure 3). The micrographs revealed that most SDF-1α coacervate was attached to the struts of the PGS scaffolds, visible as web-like structures and evenly covering the surface without blocking the pores (Figure 3A). Fluorescent images showed that SDF-1α coacervate was uniformly dispersed on the surface of flat scaffolds (Figure 3B) and in the lumen of tubular scaffolds (Figure 3C). Once applied to the surface, some SDF-1α coacervate gradually absorbed to the interstitial space of the flat scaffolds, indicating that it can be incorporated by this simple application method.

3.3. Loading efficiency and release profile

To investigate whether the coacervate can incorporate SDF-1α effectively and support its long-term sustained release, we determined the loading efficiency and *in vitro* release profile from coacervate-coated scaffolds by measuring the radioactivity of the supernatant above the scaffolds. The *in vitro* release assay indicated that the coacervate can incorporate SDF-1α with a loading efficiency of greater than 92% (day 0 of the release assay) and achieve a slow and sustained release for at least 5 weeks under static conditions and for up to 4 weeks under physiologically-relevant flow conditions (Figure 4). The static release profile showed a 94.3% loading efficiency and minimal initial burst release of 6% after 1 day, followed by a slow and linear release through day 35, after which the coacervate-coated scaffold still contained about 60% of the loaded SDF-1α. In dynamic flow, the coacervate-coated scaffold had a loading efficiency of 92.1% and a low initial burst release of 10% after 1 day, followed by relatively fast release up to day 28.

3.4. Progenitor cell migration

To evaluate migration of progenitor cells stimulated by SDF-1α released from coacervate-laden scaffolds, we used a fibrin gel embedded with fluorescence-labeled progenitor cells and quantified cell migration towards the scaffold at days 1, 4, and 7 (Figure 5A). Cross-sectional fluorescence images demonstrated that coacervate-released SDF-1α stimulates migration of both progenitor cell types upward, against gravity, towards the scaffold placed on top of the fibrin gel (Figure 5B). Cells were well dispersed throughout the gels on day 1 in both groups. Thereafter, most cells moved upward from the bottom of the gel towards SDF-1α-laden scaffolds on day 4 and were condensed near the top of the gel by day 7. Consistent with these findings, quantification of migrated cells showed no difference in cell number between SDF-1α coacervate-laden and control scaffolds through the entire depth of the gel on day 1, followed by significant decreases in cell numbers below 400 μm depths, and increases above 600 μm depths on day 7 for SDF-1α coacervate-laden scaffolds (Figures 5C and 5D). On day 7, no cbEPCs remained below 400 μm depth in SDF-1α coacervate-laden scaffolds, while above that level their numbers were 1.8-fold (at 600-800 μm) and 3-fold higher (at 800-1000 μm) than those in the control scaffolds. Similarly, bmMPC numbers in SDF-1α coacervate-laden scaffolds were 0 below 200 μm depth, and were 1.9-fold (at 600-800 μm) and 2.7-fold higher (at 800-1000 μm) than those in the control scaffolds.

3.5. Progenitor cell recruitment

To further investigate recruitment of progenitor cells into the scaffolds, we examined cell infiltration using immunofluorescent staining and dsDNA quantification. Immunofluorescent staining showed that coacervate-released SDF-1α enhanced infiltration of both progenitor cell types (Figure 6A). On day 1, both CD31 and CD90, markers for cbEPCs and bmMPCs, were co-localized on the surface in all scaffolds and were aggregated more densely in free SDF-1α scaffolds than in others. In SDF-1α coacervate-laden scaffolds, more cells were packed on the surface on day 4, followed by increased penetration into the interstitial space in a gradient organization by day 7 and continuing to day 10. In contrast, in the free SDF-1α scaffolds most cells remained tightly localized only on the surface after day 4. The DNA content of SDF-1α coacervate-laden scaffolds increased with culture time (Figure 6B). Although the free SDF-1α scaffolds had the highest number of cells on day 1, the SDF-1α coacervate-laden scaffolds had more cells compared to the free SDF-1α scaffolds on day 4 and beyond.

4. Discussion

Here we employed the coacervate, consisting of heparin and a synthetic polycation, as a delivery vehicle for SDF-1α. Heparin has been used previously for SDF-1α delivery because it is known to protect SDF-1α and facilitate its binding with CXCR4 [38, 39]. Recent heparin-based SDF-1α delivery approaches include heparin conjugated onto a functionalized hydrogel [28] or an electrospun microfibrous scaffold [25]. However, these strategies required additional modification of delivery matrices and the use of linker molecules for covalent crosslinking before incorporation of SDF-1α. On the contrary, our approach uses a strong polycation to neutralize excess negative charges on heparin molecules which drive spontaneous coacervation. Here we demonstrate that SDF-1α coacervate can also be easily incorporated and uniformly dispersed on the surface of PGS scaffolds (Figure 3) in aqueous solution without any exogenous chemicals. Since coacervation is a phase separation process, the coating method is less dependent on the surface properties of the scaffold. The water-insoluble coacervate phase will coat most solid substances contacting the solution. Furthermore, adsorbed SDF-1α coacervate did not block existing pores (Figure 3A) and created a natural SDF-1α gradient in the flat scaffolds

(Figure 3B). These results show that coacervate-laden PGS scaffolds have optimal characteristics to facilitate recruitment of progenitor cells. We expect that other heparin-binding growth factors such as FGF-2, HB-EGF, and hepatocyte growth factor (HGF), can be readily incorporated into other polymeric scaffolds using the simple coating method reported here.

A significant finding of this study is that coacervate-laden PGS scaffolds have a high loading efficiency of SDF-1α and minimal initial burst release followed by long-term sustained release under both static and flow conditions (Figure 4). Loading efficiency and sustained release are critical parameters of the therapeutic efficacy of protein delivery systems. Several SDF-1α delivery systems including microspheres [40] and hydrogels [26, 28] reported a low loading efficiency or high initial burst release under static conditions. Notably, we observed sustained release of SDF-1α under physiologically-relevant shear flow. As expected, SDF-1α released faster under flow compared to static conditions, yet release still lasted for 4 weeks. Yu *et al.* recently reported release of SDF-1α from heparin-conjugated vascular grafts under identical shear flow, however there was a high initial burst (more than 60% on day 1) and rapid release lasting only 1 week [25]. Finally, we have also shown previously that varying the polycation molecular weight allows for control over the release rate of FGF-2 from the coacervate [41]. Thus we expect that we can adjust the release rate of SDF-1α for a specific application in the future by controlling PEAD molecular weight, among other parameters. Taken together, our results suggest that coacervate-laden scaffolds can protect SDF-1α and support long-term sustained release *in vivo*.

Regarding the chemotaxis of progenitor cells via SDF-1α coacervate, our data show that human cbEPCs and bmMPCs can be targeted by a SDF-1α as they both express CXCR4 (Figure 2A). We also show that chemotaxis of both cell types increased significantly at SDF-1α dosages of 100 ng and greater (Figures 2C and 2D). These SDF-1α dosages have been shown in previous studies to induce migration and recruitment of EPCs and MPCs and neovascularization *in vivo*[18, 42]. Once applied to PGS scaffolds, SDF-1α coacervate enhanced migration of both progenitor cell types upward, against gravity, in a fibrin gel (Figure 5B). Since we used basal medium and encapsulated both cell types in the fibrin gel, similar to the native matrix, the observed cell migration must be due to the gradient of SDF-1α produced from the coacervate-laden scaffolds. It is also notable that the number of migrated cells in SDF-1α coacervate-laden scaffolds increased significantly compared to those in the control scaffolds after 4 days (Figures 5C and 5D). These results provide evidence that coacervate-laden scaffolds can induce migration of progenitor cells in the native matrix by creating a stable gradient of SDF-1α via sustained release.

In addition to enhanced migration, SDF-1α coacervate-laden PGS scaffolds also increased recruitment of both progenitor cell types over time in dynamic culture conditions (Figure 6). Compared to free SDF-1α scaffolds, SDF-1α coacervate-laden scaffolds enhanced infiltration of both cells from the surface to interstitial space of the scaffolds after day 4 (Figure 6A). Increased recruitment in free SDF-1α scaffolds on day 1 may be due to high initial release of SDF-1α, but recruited cells were densely aggregated only on the surface, and did not infiltrate the scaffold at later time points. These data indicate that applying SDF-1α in the coacervate results in better distribution of SDF-1α throughout the scaffold than applying the protein alone.

Interestingly, our results revealed that cbEPCs underwent slightly more chemotaxis than bmMPCs when stimulated by the same dosage of SDF-1α, as shown in the transwell chemotaxis (Figures 2C and 2D) and fibrin gel migration (Figures 5C and 5D) assays. Immunofluorescent staining also showed that cbEPCs ($CD31^+$ cells) penetrate deeper into

SDF-1α coacervate-laden scaffolds than bmMPCs ($CD90^+$ cells) (Figure 6A). These findings could reflect a previous study which reported that the surface expression levels of CXCR4 on bone marrow stromal cells are relatively low and this receptor may be largely found intracellularly [43]. We also observed extensive co-localization of both CD31 and CD90 fluorescent signals on the surface of SDF-1α coacervate-laden scaffolds at early time points. Since mesenchymal stem cells have been implicated in promoting the engraftment of human cord blood-derived $CD34^+$ cells post-implantation [44], we expect synergistic effects of early recruited bmMPCs on enhancing recruitment of cbEPCs *in situ*. This enhanced recruitment of both progenitor cell types suggests that SDF-1α coacervate-laden scaffolds can expedite endothelialization which is necessary for vascular grafts to prevent acute thrombosis in the early post-implantation stage. Previous *in vivo* studies demonstrated improved endothelialization in cell-free vascular grafts via SDF-1α by coating with fibronectin [45] or adsorbing onto a heparin-conjugated surface [25]. However, since these grafts used strong and slow degrading polymers, their residues are likely to limit rapid host cell infiltration and remodeling. In contrast, PGS is a fast degrading elastomer. SDF-1α coacervate-laden PGS scaffolds maintained open porous structures and stable SDF-1α gradients (Figure 3). We recently reported that heparin-coated cell-free PGS grafts enabled rapid host cell infiltration and remodeling 3 months after grafting into a rat abdominal aorta [10]. Taken together, these results suggest that PGS scaffolds combined with SDF-1α coacervate will undergo even quicker host cell infiltration and remodeling.

We recognize that site-specific homing of these progenitor cells is required for vascular remodeling in SDF-1α coacervate-laden PGS grafts. Our previous study indicated that PGS grafts alone underwent host remodeling to form functional neoarteries with proper cellular organization including an endothelialized lumen, smooth muscle-rich medial layer, and fibroblast-filled adventitia [10]. We speculate that the local biomechanical and biochemical niche likely contributed to cell differentiation and maintenance of proper phenotype. If necessary, this process might be enhanced by separation of the lumen from the wall using a PGS membrane to form an endothelial compartment and a smooth muscle compartment, each with its own growth factor cues.

Here we showed enhanced recruitment of human progenitor cells using *in vitro* assays, thus the application of this approach in animals would be the next step to assess efficacy. To date, no animal models to assess human progenitor cell recruitment by SDF-1α for vascular regeneration have been reported. Several published SDF-1α delivery systems have demonstrated progenitor cell recruitment in animal models, however, most of them were implanted in the subcutaneous region [22-24, 28]. A recent study has demonstrated enhanced recruitment of both endothelial and smooth muscle progenitor cells via SDF-1α immobilized vascular graft after implantation in rat carotid artery [25]. The results reported here are distinctive in that the focus is recruitment of human cbEPCs and bmMPCs via controlled release of SDF-1α in cell-free vascular grafts. Several studies have shown that SDF-1α and its receptor CXCR4 enhance homing and repopulation of human stem cells in immune-deficient mice [17, 46]. Thus, immune-deficient mice might be a good candidate model for these assessments since human and murine SDF-1α are cross-reactive [47]. The origin and type of host cells induced by SDF-1α and their roles in host remodeling require further investigation.

Cost is an important factor for clinical translation. Most growth factors are expensive; therefore maintenance of bioactivity for maximal *in vivo* efficacy is critical. The high efficiency of the coacervate enables the use of minute doses and a single administration. For example, the coacervate delivery systems typically only need nanogram growth factors to achieve sustained physiological activity in vivo [32, 34]. In comparison, free growth factor therapies often require multiple administrations of microgram and even milligram quantities

to obtain a significant effect in animal models. We therefore anticipate that the added cost of SDF-1α in future vascular grafts will not be prohibitive.

The coacervate delivery system is designed for heparin-binding growth factors. There are over 400 proteins that bind heparin [48], many of which are critical for vascular tissue engineering including VEGF, platelet-derived growth factor (PDGF), and HGF. It is worth noting that the potential applications of coacervate-laden scaffolds are not limited to blood vessels. FGF-2 and HB-EGF released from the coacervate enhanced angiogenesis [32, 33] and wound healing [34], respectively. Coacervate-delivered sonic hedgehog also shows promise for cardiac repair [49]. Therefore, we expect that coacervate-laden scaffolds will be useful in many areas of soft tissue engineering including myocardium, skeletal muscle, connective tissue, and tissues of the digestive tract.

5. Conclusion

In summary, we developed a new controlled release system for SDF-1α consisting of a coacervate-coated PGS scaffold. This system demonstrated the following advantages: (1) high loading efficiency of SDF-1α with maintained bioactivity; (2) long-term sustained release of SDF-1α under both static and physiologically-relevant shear flow conditions with a minimal initial burst release; (3) ease of SDF-1α incorporation; and (4) open porous structures and uniform distribution of SDF-1α on the scaffolds. The coacervate-laden PGS scaffolds enhanced migration and recruitment of both human cbEPCs and bmMPCs by maintaining a stable SDF-1α gradient. These results suggest that SDF-1α coacervate-laden PGS scaffolds can accelerate host progenitor cell migration and recruitment for *in situ* vascular regeneration.

Acknowledgments

The authors thank Dr. Joyce Bischoff at Children's Hospital in Boston for kindly providing human cbEPCs and bmMPCs. Research reported in this publication was supported by the National Heart, Lung, And Blood Institute of the National Institutes of Health under Award Number R01HL089658 and the American Heart Association Established Investigator Award #12EIA9020016. The content is solely the responsibility of the authors and does not necessarily represent the official views of the National Institutes of Health.

References

1. Weinberg CB, Bell E. A blood vessel model constructed from collagen and cultured vascular cells. Science. 1986; 231:397–400. [PubMed: 2934816]
2. Niklason LE, Gao J, Abbott WM, Hirschi KK, Houser S, Marini R, et al. Functional arteries grown in vitro. Science. 1999; 284:489–93. [PubMed: 10205057]
3. L'Heureux N, Paquet S, Labbe R, Germain L, Auger FA. A completely biological tissue-engineered human blood vessel. Faseb J. 1998; 12:47–56. [PubMed: 9438410]
4. Dahl SL, Kypson AP, Lawson JH, Blum JL, Strader JT, Li Y, et al. Readily available tissue-engineered vascular grafts. Sci Transl Med. 2011; 3:68ra9.
5. Quint C, Kondo Y, Manson RJ, Lawson JH, Dardik A, Niklason LE. Decellularized tissue-engineered blood vessel as an arterial conduit. Proc Natl Acad Sci U S A. 2011; 108:9214–9. [PubMed: 21571635]
6. Matsumura G, Hibino N, Ikada Y, Kurosawa H, Shin'oka T. Successful application of tissue engineered vascular autografts: clinical experience. Biomaterials. 2003; 24:2303–8. [PubMed: 12699667]
7. Shin'oka T, Matsumura G, Hibino N, Naito Y, Watanabe M, Konuma T, et al. Midterm clinical result of tissue-engineered vascular autografts seeded with autologous bone marrow cells. J Thorac Cardiovasc Surg. 2005; 129:1330–8. [PubMed: 15942574]

8. Hibino N, Villalona G, Pietris N, Duncan DR, Schoffner A, Roh JD, et al. Tissue-engineered vascular grafts form neovessels that arise from regeneration of the adjacent blood vessel. Faseb J. 2011; 25:2731–9. [PubMed: 21566209]
9. Roh JD, Sawh-Martinez R, Brennan MP, Jay SM, Devine L, Rao DA, et al. Tissue-engineered vascular grafts transform into mature blood vessels via an inflammation-mediated process of vascular remodeling. Proc Natl Acad Sci U S A. 2010; 107:4669–74. [PubMed: 20207947]
10. Wu W, Allen RA, Wang Y. Fast-degrading elastomer enables rapid remodeling of a cell-free synthetic graft into a neoartery. Nat Med. 2012; 18:1148–53. [PubMed: 22729285]
11. Asahara T, Murohara T, Sullivan A, Silver M, van der Zee R, Li T, et al. Isolation of putative progenitor endothelial cells for angiogenesis. Science. 1997; 275:964–7. [PubMed: 9020076]
12. Kaushal S, Amiel GE, Guleserian KJ, Shapira OM, Perry T, Sutherland FW, et al. Functional small-diameter neovessels created using endothelial progenitor cells expanded ex vivo. Nat Med. 2001; 7:1035–40. [PubMed: 11533707]
13. Schmidt D, Breymann C, Weber A, Guenter CI, Neuenschwander S, Zund G, et al. Umbilical cord blood derived endothelial progenitor cells for tissue engineering of vascular grafts. Ann Thorac Surg. 2004; 78:2094–8. [PubMed: 15561042]
14. Melero-Martin JM, Khan ZA, Picard A, Wu X, Paruchuri S, Bischoff J. In vivo vasculogenic potential of human blood-derived endothelial progenitor cells. Blood. 2007; 109:4761–8. [PubMed: 17327403]
15. Melero-Martin JM, De Obaldia ME, Kang SY, Khan ZA, Yuan L, Oettgen P, et al. Engineering robust and functional vascular networks in vivo with human adult and cord blood-derived progenitor cells. Circ Res. 2008; 103:194–202. [PubMed: 18556575]
16. Allen P, Melero-Martin J, Bischoff J. Type I collagen, fibrin and PuraMatrix matrices provide permissive environments for human endothelial and mesenchymal progenitor cells to form neovascular networks. J Tissue Eng Regen Med. 2011; 5:e74–86. [PubMed: 21413157]
17. Peled A, Petit I, Kollet O, Magid M, Ponomaryov T, Byk T, et al. Dependence of human stem cell engraftment and repopulation of NOD/SCID mice on CXCR4. Science. 1999; 283:845–8. [PubMed: 9933168]
18. Yamaguchi J, Kusano KF, Masuo O, Kawamoto A, Silver M, Murasawa S, et al. Stromal cell-derived factor-1 effects on ex vivo expanded endothelial progenitor cell recruitment for ischemic neovascularization. Circulation. 2003; 107:1322–8. [PubMed: 12628955]
19. De Falco E, Porcelli D, Torella AR, Straino S, Iachininoto MG, Orlandi A, et al. SDF-1 involvement in endothelial phenotype and ischemia-induced recruitment of bone marrow progenitor cells. Blood. 2004; 104:3472–82. [PubMed: 15284120]
20. Misra P, Lebeche D, Ly H, Schwarzkopf M, Diaz G, Hajjar RJ, et al. Quantitation of CXCR4 expression in myocardial infarction using 99mTc-labeled SDF-1alpha. J Nucl Med. 2008; 49:963–9. [PubMed: 18483105]
21. McQuibban GA, Butler GS, Gong JH, Bendall L, Power C, Clark-Lewis I, et al. Matrix metalloproteinase activity inactivates the CXC chemokine stromal cell-derived factor-1. J Biol Chem. 2001; 276:43503–8. [PubMed: 11571304]
22. Schantz JT, Chim H, Whiteman M. Cell guidance in tissue engineering: SDF-1 mediates site-directed homing of mesenchymal stem cells within three-dimensional polycaprolactone scaffolds. Tissue Eng. 2007; 13:2615–24. [PubMed: 17961003]
23. Thevenot PT, Nair AM, Shen J, Lotfi P, Ko CY, Tang L. The effect of incorporation of SDF-1alpha into PLGA scaffolds on stem cell recruitment and the inflammatory response. Biomaterials. 2010; 31:3997–4008. [PubMed: 20185171]
24. Ko IK, Ju YM, Chen T, Atala A, Yoo JJ, Lee SJ. Combined systemic and local delivery of stem cell inducing/recruiting factors for in situ tissue regeneration. Faseb J. 2012; 26:158–68. [PubMed: 21965595]
25. Yu J, Wang A, Tang Z, Henry J, Li-Ping Lee B, Zhu Y, et al. The effect of stromal cell-derived factor-1alpha/heparin coating of biodegradable vascular grafts on the recruitment of both endothelial and smooth muscle progenitor cells for accelerated regeneration. Biomaterials. 2012; 33:8062–74. [PubMed: 22884813]

26. He X, Ma J, Jabbari E. Migration of marrow stromal cells in response to sustained release of stromal-derived factor-1alpha from poly(lactide ethylene oxide fumarate) hydrogels. Int J Pharm. 2010; 390:107–16. [PubMed: 20219655]
27. Kimura Y, Tabata Y. Controlled release of stromal-cell-derived factor-1 from gelatin hydrogels enhances angiogenesis. J Biomater Sci Polym Ed. 2010; 21:37–51. [PubMed: 20040152]
28. Prokoph S, Chavakis E, Levental KR, Zieris A, Freudenberg U, Dimmeler S, et al. Sustained delivery of SDF-1alpha from heparin-based hydrogels to attract circulating pro-angiogenic cells. Biomaterials. 2012; 33:4792–800. [PubMed: 22483246]
29. Purcell BP, Elser JA, Mu A, Margulies KB, Burdick JA. Synergistic effects of SDF-1alpha chemokine and hyaluronic acid release from degradable hydrogels on directing bone marrow derived cell homing to the myocardium. Biomaterials. 2012; 33:7849–57. [PubMed: 22835643]
30. Huang YC, Liu TJ. Mobilization of mesenchymal stem cells by stromal cell-derived factor-1 released from chitosan/tripolyphosphate/fucoidan nanoparticles. Acta Biomater. 2012; 8:1048–56. [PubMed: 22200609]
31. Chu H, Johnson NR, Mason NS, Wang Y. A [polycation:heparin] complex releases growth factors with enhanced bioactivity. J Control Release. 2011; 150:157–63. [PubMed: 21118705]
32. Chu H, Gao J, Chen CW, Huard J, Wang Y. Injectable fibroblast growth factor-2 coacervate for persistent angiogenesis. Proc Natl Acad Sci U S A. 2011; 108:13444–9. [PubMed: 21808045]
33. Chu H, Chen CW, Huard J, Wang Y. The effect of a heparin-based coacervate of fibroblast growth factor-2 on scarring in the infarcted myocardium. Biomaterials. 2013; 34:1747–56. [PubMed: 23211448]
34. Johnson NR, Wang Y. Controlled delivery of heparin-binding EGF-like growth factor yields fast and comprehensive wound healing. J Control Release. 2013; 166:124–9. [PubMed: 23154193]
35. Wang Y, Ameer GA, Sheppard BJ, Langer R. A tough biodegradable elastomer. Nat Biotechnol. 2002; 20:602–6. [PubMed: 12042865]
36. Gao J, Crapo PM, Wang Y. Macroporous elastomeric scaffolds with extensive micropores for soft tissue engineering. Tissue Eng. 2006; 12:917–25. [PubMed: 16674303]
37. Lee KW, Wang Y. Elastomeric PGS scaffolds in arterial tissue engineering. J Vis Exp. 2011
38. Amara A, Lorthioir O, Valenzuela A, Magerus A, Thelen M, Montes M, et al. Stromal cell-derived factor-1alpha associates with heparan sulfates through the first beta-strand of the chemokine. J Biol Chem. 1999; 274:23916–25. [PubMed: 10446158]
39. Murphy JW, Cho Y, Sachpatzidis A, Fan C, Hodsdon ME, Lolis E. Structural and functional basis of CXCL12 (stromal cell-derived factor-1 alpha) binding to heparin. J Biol Chem. 2007; 282:10018–27. [PubMed: 17264079]
40. Cross DP, Wang C. Stromal-derived factor-1 alpha-loaded PLGA microspheres for stem cell recruitment. Pharm Res. 2011; 28:2477–89. [PubMed: 21614634]
41. Zern BJ, Chu H, Wang Y. Control growth factor release using a self-assembled [polycation:heparin] complex. PLoS One. 2010; 5:e11017. [PubMed: 20543985]
42. Ponte AL, Marais E, Gallay N, Langonne A, Delorme B, Herault O, et al. The in vitro migration capacity of human bone marrow mesenchymal stem cells: comparison of chemokine and growth factor chemotactic activities. Stem Cells. 2007; 25:1737–45. [PubMed: 17395768]
43. Wynn RF, Hart CA, Corradi-Perini C, O'Neill L, Evans CA, Wraith JE, et al. A small proportion of mesenchymal stem cells strongly expresses functionally active CXCR4 receptor capable of promoting migration to bone marrow. Blood. 2004; 104:2643–5. [PubMed: 15251986]
44. Noort WA, Kruisselbrink AB, in't Anker PS, Kruger M, van Bezooijen RL, de Paus RA, et al. Mesenchymal stem cells promote engraftment of human umbilical cord blood-derived CD34(+) cells in NOD/SCID mice. Exp Hematol. 2002; 30:870–8. [PubMed: 12160838]
45. De Visscher G, Mesure L, Meuris B, Ivanova A, Flameng W. Improved endothelialization and reduced thrombosis by coating a synthetic vascular graft with fibronectin and stem cell homing factor SDF-1alpha. Acta Biomater. 2012; 8:1330–8. [PubMed: 21964214]
46. Lapidot T. Mechanism of human stem cell migration and repopulation of NOD/SCID and B2mnull NOD/SCID mice. The role of SDF-1/CXCR4 interactions. Ann N Y Acad Sci. 2001; 938:83–95. [PubMed: 11458529]

47. Nagasawa T, Tachibana K, Kishimoto T. A novel CXC chemokine PBSF/SDF-1 and its receptor CXCR4: their functions in development, hematopoiesis and HIV infection. Semin Immunol. 1998; 10:179–85. [PubMed: 9653044]

48. Ori A, Wilkinson MC, Fernig DG. A systems biology approach for the investigation of the heparin/heparan sulfate interactome. J Biol Chem. 2011; 286:19892–904. [PubMed: 21454685]

49. Johnson NR, Wang Y. Controlled delivery of sonic hedgehog morphogen and its potential for cardiac repair. PLoS One. 2013; 8:e63075. [PubMed: 23690982]

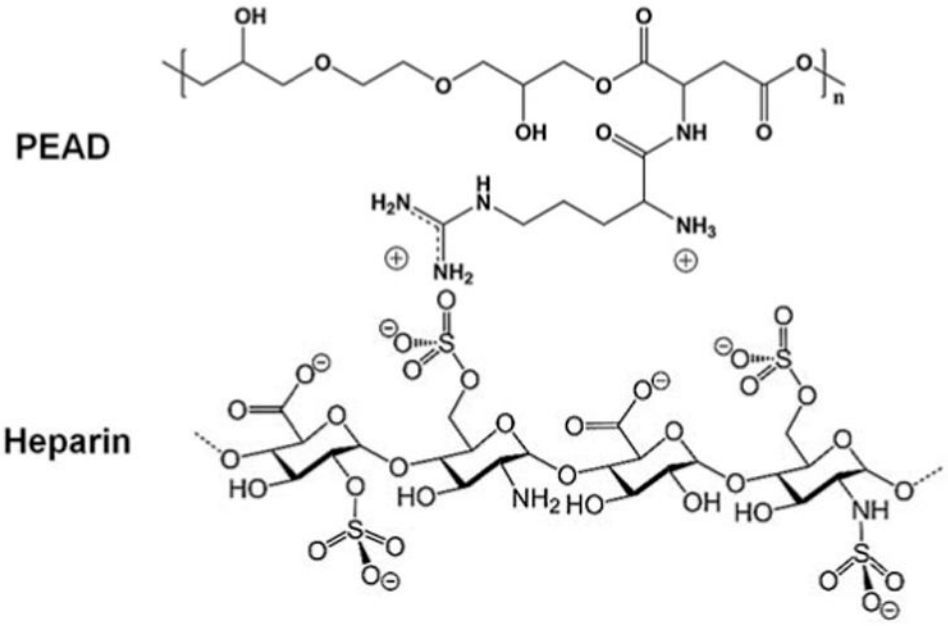

Figure 1.
Composition of a self-assembled coacervate.

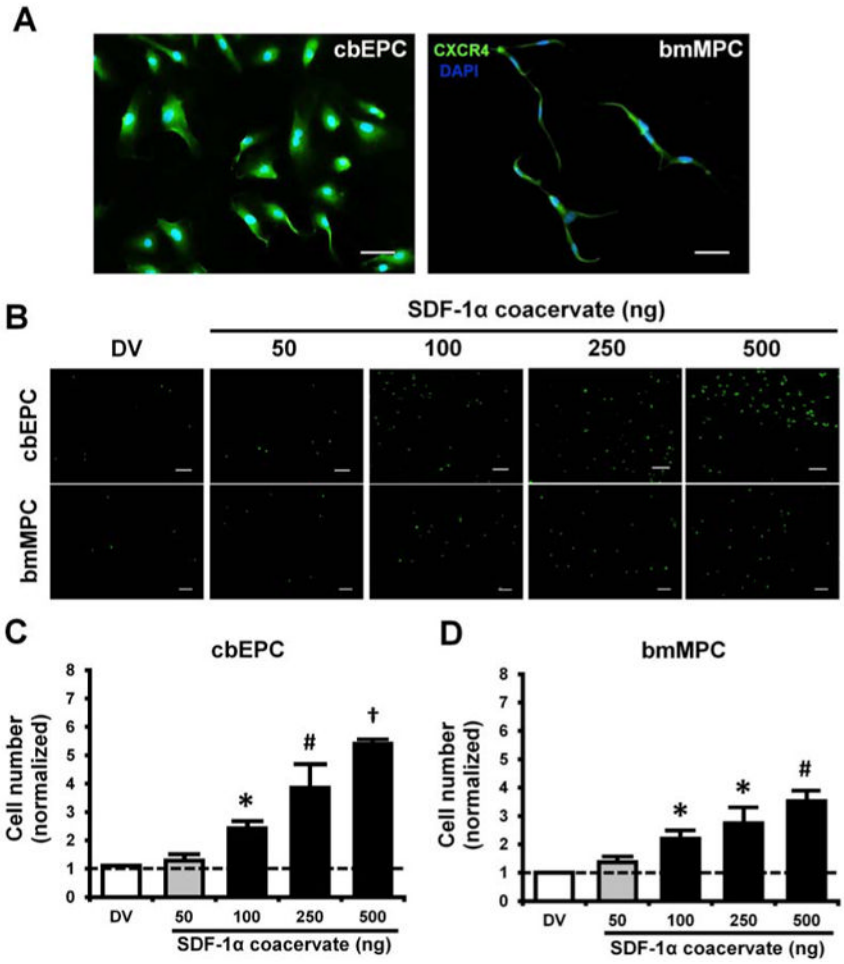

Figure 2.

Characterization and chemotaxis of progenitor cells. (A) CXCR4 expression of cbEPCs and bmMPCs, (B) Fluorescent images of migrated progenitor cells on the bottom of transwell insert membrane. Scale bar = 200 μm. (C) and (D) Quantification of migrated cells. Cell numbers in each group were normalized by those in basal medium group. *$p < 0.05$ (compared to DV and 50), $^{\#}p < 0.05$ (compared to DV, 50, and 100), $^{\dagger}p < 0.05$ (compared to all other groups) ($n = 4$).

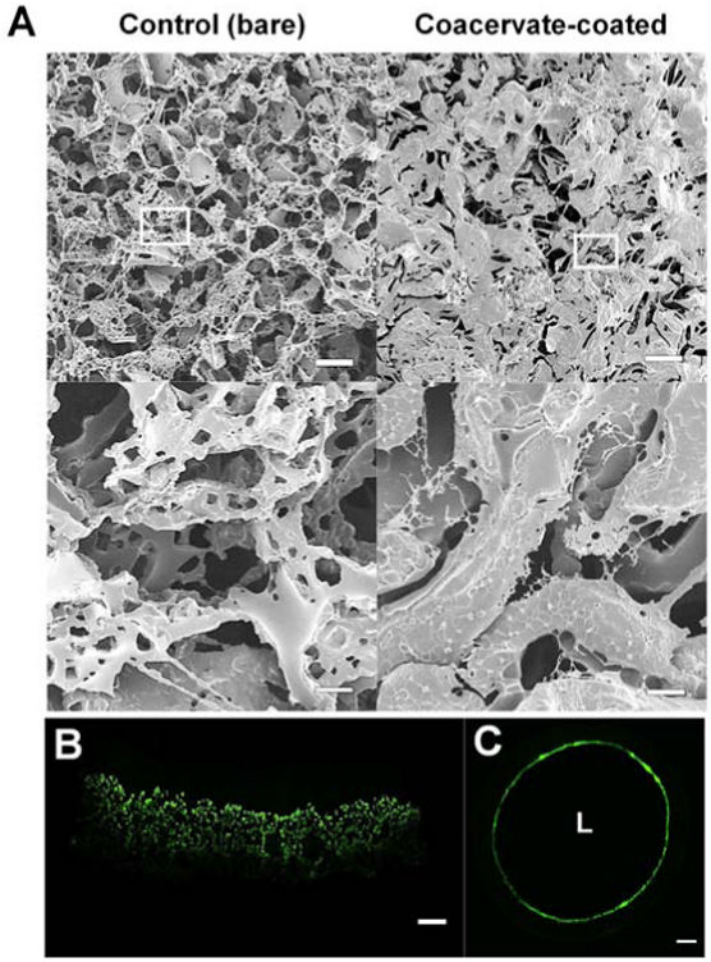

Figure 3.

Incorporation and distribution of SDF-1α coacervate in PGS scaffolds. (A) Scanning electron micrographs of empty (control) and SDF-1α coacervate-coated scaffolds. Bottom row represents partial magnification of the box shown in top row. Scale bar = 100 μm (top row) and 10 μm (bottom row). (B) and (C) distribution of the fluorescence-labeled SDF-1α coacervate in the flat and tubular scaffolds. Scale bar = 500 μm (all). L: lumen of the scaffold.

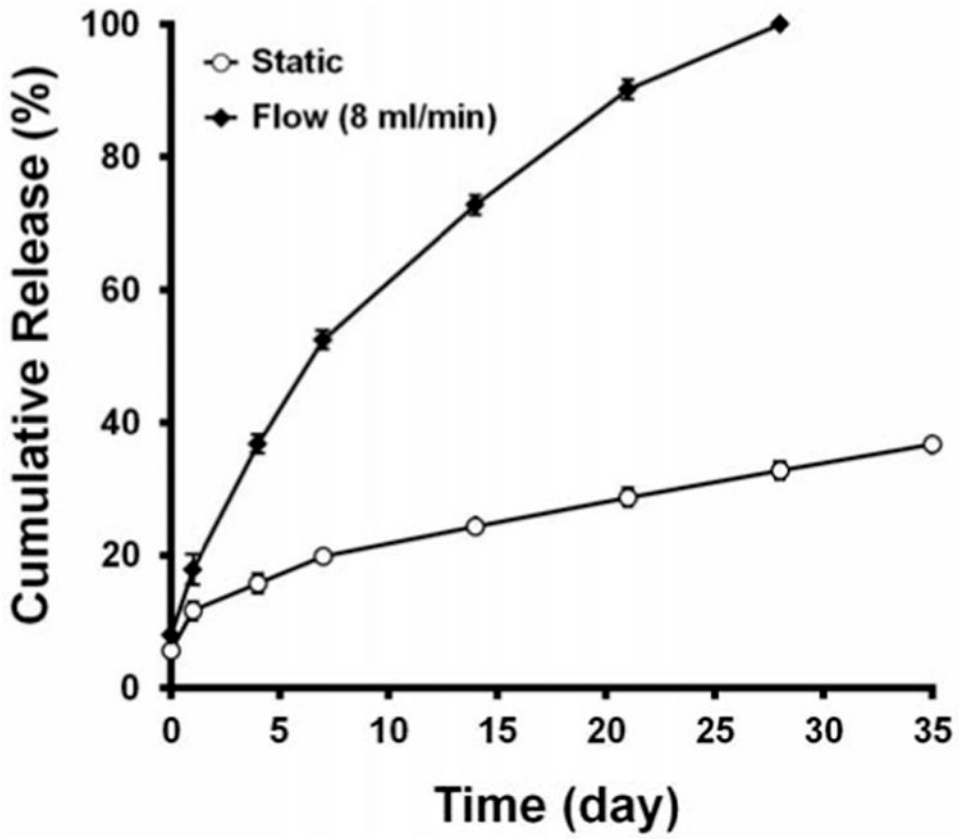

Figure 4.
In vitro release profiles of SDF-1α from the coacervate-coated scaffolds in static and flow conditions.

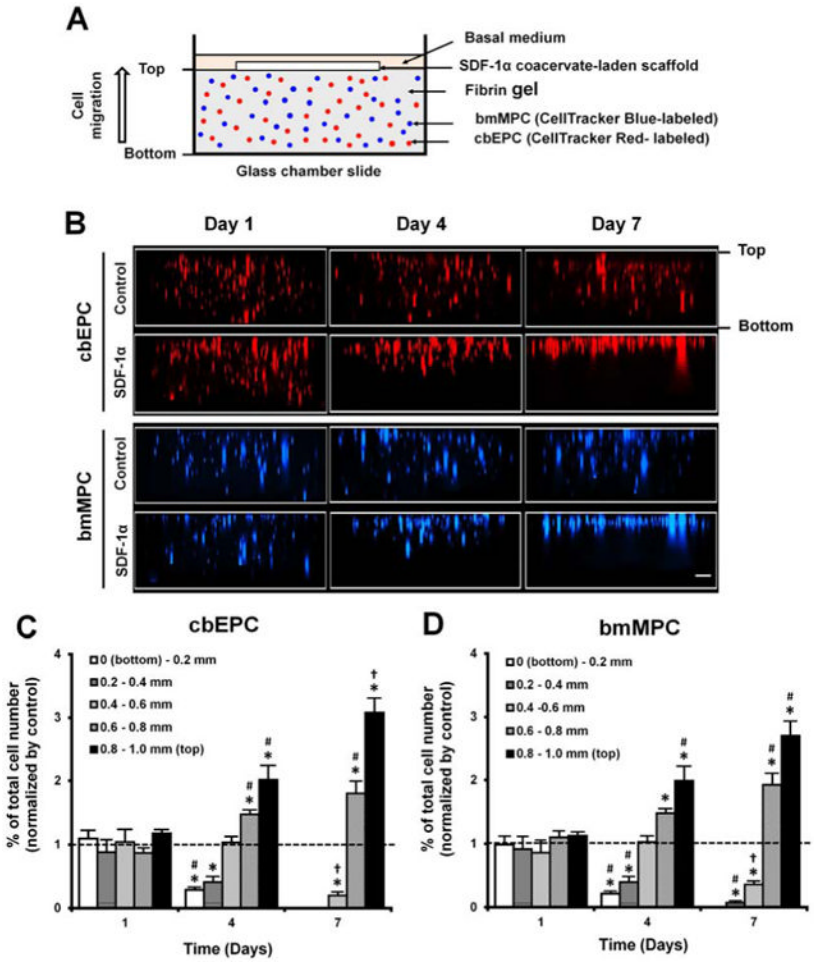

Figure 5.

Migration of progenitor cells from SDF-1α coacervate-laden scaffolds. (A) Schematic of the cell migration assay. (B) Cross-sectional images of fibrin gels. The difference in migration of fluorescence-labeled progenitor cells in response to empty scaffold (Control) and SDF-1α coacervate-laden scaffold (SDF-1α). (C) Quantification of vertically migrated cells in the fibrin gel of SDF-1α coacervate-laden scaffolds. Cell numbers at each depth in both groups were normalized by total number of cells in the entire gel. Final normalized cell numbers in SDF-1α group were divided into those in control group and represented as a fold difference vs. control. Dashed line represents the normalized cell numbers in control group. $^{*}p < 0.05$ (compared to control), $^{\#}p < 0.05$ (compared to day 1), $^{\dagger}p < 0.05$ (compared to days 1 and 4).

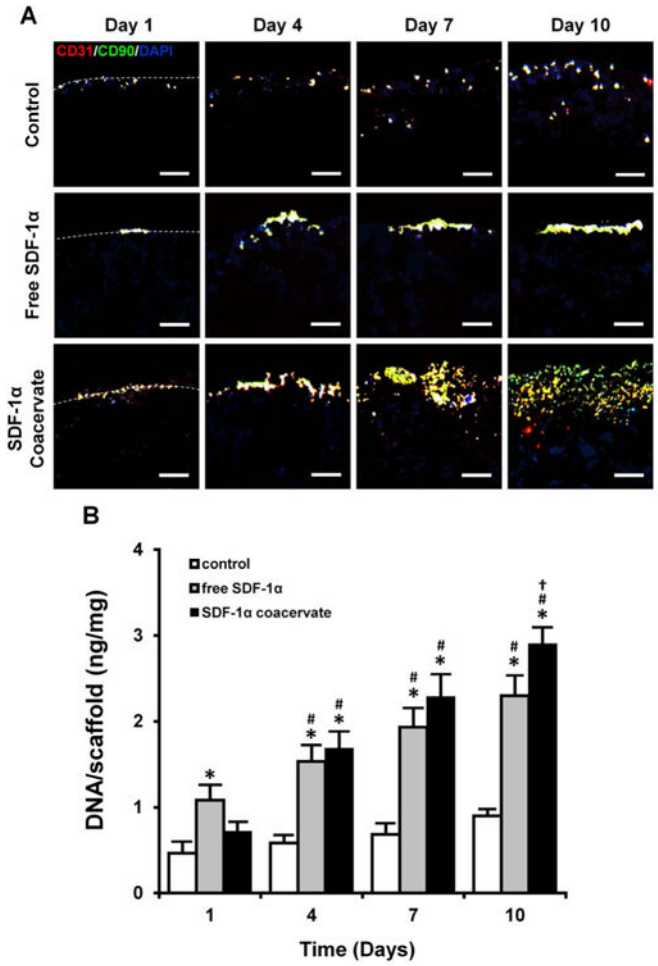

Figure 6.

Recruitment of progenitor cells into the SDF-1α coacervate-laden scaffolds. (A) Immunofluorescent staining for CD31 (cbEPC marker, red), CD90 (bmMPC marker, green), and DAPI (nuclei, blue). Dashed lines represent the border between the outer region (top) and the scaffolds (bottom). Scale bar = 100 μm (all). (B) Quantification of the number of cells in scaffolds. The number of cells was normalized by the wet weight of scaffolds. *$p < 0.05$ (compared to control), $^{\#}p < 0.05$ (compared to day 1), $^{\dagger}p < 0.05$ (compared to day 4) ($n = 4$).

Table 1

Compositions of experimental groups for chemotaxis assay. BM: basal medium. DV: delivery vehicle (coacervate only).

	BM	DV	SDF-1α coacervate (ng)			
			50	100	250	500
Heparin (10 mg/ml) (μl)	-	5	5	5	5	5
SDF-1α (50 ng/μl) (μl)	-	-	1	2	5	10
PEAD (10 mg/ml) (μl)	-	25	25	25	25	25
DI water (μl)	40	10	9	8	5	-